THE JOURNAL OF BIOLOGICAL CHEMISTRY VOL. 288, NO. 47, pp. 33953–33965, November 22, 2013

The Inhibitory Effects of a Rhamnogalacturonan I (RG-I) Domain from Ginseng Pectin on Galectin-3 and Its Structure-Activity Relationship*[S]

Received for publication, May 5, 2013, and in revised form, September 23, 2013 Published, JBC Papers in Press, October 7, 2013, DOI 10.1074/jbc.M113.482315

Xiaoge Gao, Yuan Zhi, Lin Sun, Xiaoxia Peng, Tao Zhang, Huiting Xue, Guihua Tai[1], and Yifa Zhou[2]

From the School of Life Sciences, Northeast Normal University, Changchun 130024, China

Background: Structural elements in pectin that inhibit galectin-3, a β-galactoside-binding protein associated with cancer progression, are poorly defined.
Results: Both backbone and side chains of pectin RG-I-4 were important for its anti-galectin-3 activity.
Conclusion: High activity of RG-I-4 was due to cooperation between short β1,4-galactan side chains.
Significance: The results are valuable for producing highly active pectin-based galectin-3 inhibitors.

Pectin has been shown to inhibit the actions of galectin-3, a β-galactoside-binding protein associated with cancer progression. The structural features of pectin involved in this activity remain unclear. We investigated the effects of different ginseng pectins on galectin-3 action. The rhamnogalacturonan I-rich pectin fragment, RG-I-4, potently inhibited galectin-3-mediated hemagglutination, cancer cell adhesion and homotypic aggregation, and binding of galectin-3 to T-cells. RG-I-4 specifically bound to the carbohydrate recognition domain of galectin-3 with a dissociation constant of 22.2 nM, which was determined by surface plasmon resonance analysis. The structure-activity relationship of RG-I-4 was investigated by modifying the structure through various enzymatic and chemical methods followed by activity tests. The results showed that (*a*) galactan side chains were essential to the activity of RG-I-4, whereas arabinan side chains positively or negatively regulated the activity depending on their location within the RG-I-4 molecule. (*b*) The activity of galactan chain was proportional to its length up to 4 Gal residues and largely unchanged thereafter. (*c*) The majority of galactan side chains in RG-I-4 were short with low activities. (*d*) The high activity of RG-I-4 resulted from the cooperative action of these side chains. (*e*) The backbone of the molecule was very important to RG-I-4 activity, possibly by maintaining a structural conformation of the whole molecule. (*f*) The isolated backbone could bind galectin-3, which was insensitive to lactose treatment. The novel discovery that the side chains and backbone play distinct roles in regulating RG-I-4 activity is valuable for producing highly active pectin-based galectin-3 inhibitors.

Galectin-3 is the only chimeric member of the galectin family, which is characterized by a conserved carbohydrate recognition domain (CRD)[3] that specifically binds to β-galactosides (1–3). Galectin-3 has a C-terminal CRD connected to a long N-terminal proline- and glycine-rich domain (1). X-ray crystal structure analysis has revealed that galectin-3 CRD is composed of a five-stranded and a six-stranded β-sheet in a β-sandwich arrangement. The binding groove is long enough to hold a linear tetrasaccharide (4). Galectin-3 can oligomerize in the presence of multivalent carbohydrate ligands (5). This self-association property depends on the N-terminal domain (5). Oligomerization of galectin-3 is essential for some of its biological functions (6).

Galectin-3 is involved in various biological processes, such as cell-cell interactions, proliferation, differentiation, apoptosis, and mRNA splicing, and is associated with different pathologic conditions including cancer (1, 3, 7, 8). Galectin-3 is highly expressed in a subset of metastatic cancer cells in comparison with benign or normal cells and is a potential diagnostic and/or prognostic marker for some types of cancers (9). The role of galectin-3 in cancer progression and metastasis has been extensively studied. Overexpression of galectin-3 protects cancer cells from apoptosis in the presence of ultraviolet radiation or antitumor drugs (10). Interaction of galectin-3 with the cancer-associated Thomsen-Friedenreich glycoantigen mediates the initial adhesion of cancer cells to the vascular wall and subsequent tumor cell homotypic aggregation at the site of primary attachment to the endothelium (11). Galectin-3 acts as a chemoattractant and induces endothelial cell migration and tube formation, which are two important steps in tumor angiogenesis (12). Galectin-3 may also facilitate immune evasion of tumor cells by binding to T-cell receptors, which leads to inhibition of T-cell activation and apoptosis of T-cells (13).

Because galectin-3 contributes to tumor progression, numerous studies have focused on the development of specific galectin-3 inhibitors including peptide antagonists (14), lactu-

* This work was supported by National Natural Science Foundation of China Grants 31370805 and 31170770, Chinese New Drug Creation and Manufacturing Program Grant 2012ZX09502001-001, and Fundamental Research Funds for the Central Universities Grant 12SSXM005.
[S] This article contains supplemental Figs. S1–S3 and Table S1.
[1] To whom correspondence may be addressed. Tel.: 86-431-8509-9165; Fax: 86-431-8509-8212; E-mail: taigh477@nenu.edu.cn.
[2] To whom correspondence may be addressed. Tel.: 86-431-8509-8212; Fax: 86-431-8509-8212; E-mail: zhouyf383@nenu.edu.cn.

[3] The abbreviations used are: CRD, carbohydrate recognition domain; G3H, galectin-3-mediated hemagglutination; MIC, minimum inhibitory concentration; AG, arabinogalactan; HG, homogalacturonan; GalA, galacturonic acid; Gal, galactose; Ara, arabinose; Rha, rhamnose; RG-I, rhamnogalacturonan I; ASF, asialofetuin; MCP, modified citrus pectin; endo-PG, endopolygalacturonase; SPR, surface plasmon resonance; DTAF, 5-(4,6-dichlorotriazinyl)aminofluorescein; LacNAc, *N*-acetyllactosamine.

lose amines (15), and galactose-based inhibitors (16, 17). In addition to these synthetic molecules, a natural product, pectin, has emerged as a good source for generating high affinity galectin-3 inhibitors with low toxicity. Several pectins and pectic polysaccharides, such as modified citrus pectin (MCP), swallow root pectin, *Hemidesmus* pectin, black cumin pectin, *Andrographis* pectin, and okra pectin have been reported to possess anti-galectin-3 activities (18–22). Among these pectin-based inhibitors, MCP has attracted special attention. Studies from several groups have shown that MCP inhibits multiple steps of tumor metastasis via inhibition of galectin-3 including inhibition of cancer cell adhesion, homotypic aggregation, invasion, clonogenic survival, angiogenesis, sensitization of neoplastic cells to apoptosis induced by chemotherapeutic agents, and correction of the impaired function of tumor-infiltrating lymphocytes (20, 23–28).

Although interaction between pectin and galectin-3 has been recognized for some time, the structural features of pectin that contribute to that interaction are poorly understood. One hypothesis that has been proposed in the literature is that the galactose (Gal) residues in pectin facilitate interaction with galectin-3 (19, 23, 24). However, there are many Gal-containing pectins in nature, and only a few have been shown to interact with galectin-3. Clearly, the presence of Gal residues alone is insufficient. Pectin has a very complex structure. It usually contains galacturonic acid (GalA), Gal, arabinose (Ara), and rhamnose (Rha) residues. The content and linkages of each residue differ between plants and can vary within different parts of the same plant. This does not mean that the residues are randomly linked. In fact, they are organized into distinct structural elements or domains, such as galactan/arabinogalactan (AG), homogalacturonan (HG), rhamnogalacturonan I (RG-I), rhamnogalacturonan II, and xylogalacturonan. Each element or domain differs considerably between species (29). Gunning *et al.* (30) reported that β1,4-galactan derived from potato pectin specifically recognized galectin-3. Our research group isolated β1,4-galactan fragments from MCP. We found that the chain termini and not the internal region regulated interactions with galectin-3 (31). Despite these findings, the structure-activity relationship remains far from clear due to the lack of structurally defined pectin fractions or fragments. In this regard, our research group isolated and characterized four HG-rich and four AG-rich pectins from ginseng and five RG-I-rich pectin fragments from endo-PG-treated ginseng pectin (32–34). In the present study, we examined the inhibitory effects of these pectins and fragments on galectin-3-mediated activities and identified one of the RG-I-rich pectin fragments as a potent inhibitor of galectin-3. Additional structure-activity studies demonstrated that, besides Gal residues, both the backbone and the side chains of this fragment were important for inhibition of galectin-3.

EXPERIMENTAL PROCEDURES

Reagents

Fetuin was purchased from Sigma (F2379). Asialofetuin (ASF) was prepared by mild acid hydrolysis of fetuin in 0.05 M H_2SO_4 at 80 °C for 1 h. Lactose-Sepharose CL-6B was prepared with lactose and Sepharose CL-6B according to a previously published protocol (35). Recombinant human galectin-3 and GST-galectin-3 were prepared according to our previous publication (36). The enzymes endo-α1,5-L-arabinanase, endo-β1,4-D-galactanase, and α-L-arabinofuranosidase were purchased from Megazyme. The enzymes polygalacturonase (EC 3.2.1.15 from *Aspergillus niger*) and β-D-galactosidase were from Sigma. The fluorescent dye 5-(4,6-dichlorotriazinyl)aminofluorescein (DTAF) was obtained from Invitrogen. A monoclonal antibody against β1,4-galactan (LM5) was a generous gift from Professor J. Paul Knox (Faculty of Biological Sciences, Centre for Plant Sciences, University of Leeds, Leeds, UK). Other reagents were of analytical grade or better.

Pectic Polysaccharide Samples

Pectic galactan and RG-I derived from potato were purchased from Megazyme. AG derived from larch wood was obtained from Sigma-Aldrich. MCP was prepared from citrus pectin (Sigma, P9135) by pH modification according to published methods (18, 31). MCP and all pectic samples used in this study were normalized by dialysis against distilled water followed by lyophilization. Ginseng pectin fractions WGPA-1-HG, WGPA-2-HG, WGPA-3-HG, WGPA-4-HG, WGPA-1-RG, WGPA-2-RG, WGPA-3-RG, and WGPA-4-RG were prepared from the roots of *Panax ginseng* C. A. Mey according to our published protocol (32, 33). Ginseng RG-I fragments RG-I-2, RG-I-3B, and RG-I-4 were prepared from endo-PG-digested ginseng pectin according to our previous publication (34). The backbone of RG-I-4, referred to as RG-I-4-RG, was prepared by partial hydrolysis of RG-I-4 with 0.1 M trifluoroacetic acid at 80 °C for 16 h followed by dialysis against distilled water and lyophilization.

Modification of RG-I-4

Enzymatic Digestion—Enzymatic digestion with endo-α1,5-L-arabinanase, α-L-arabinofuranosidase, endo-β1,4-D-galactanase, or β-D-galactosidase was performed according to published methods (37). In each case, the control sample was treated similarly to the test samples but without enzyme. The digests were dialyzed extensively and lyophilized.

β-Elimination—β-Elimination was performed according to a published protocol (38). Briefly, 5 mg/ml RG-I-4, which was dissolved in 0.2 M sodium borate buffer (pH 7.3), was heated for 4 h at 120 °C. The products were dialyzed and lyophilized.

De-esterification—De-esterification was performed based on the literature (32). Briefly, 10 mg/ml RG-I-4 was treated with 0.1 M NaOH at 4 °C for 4 h followed by neutralization and desalting on a Sephadex G-25 column (2 × 20 cm).

Preparation of Galacto-oligosaccharides

All galacto-oligosaccharides were prepared from potato galactan. Oligosaccharides A–E were prepared by enzymatic digestion. Briefly, 200 mg of potato galactan, which was dissolved in 20 ml of 50 mM sodium acetate buffer (pH 4.5), was incubated with 0.3 unit/ml endo-β1,4-D-galactanase from *A. niger* at 30 °C for 24 h. The digest was boiled for 5 min, centrifuged, loaded onto a Bio-Gel P-2 column (2 × 90 cm), and eluted with distilled water at a flow rate of 0.15 ml/min. The

eluate was collected at 4.5 ml/tube, analyzed by the phenol-sulfuric acid assay (32), and pooled as shown in supplemental Fig. S1a.

Oligosaccharides F–M were prepared by partial acid hydrolysis. Briefly, 1 g of potato galactan was dissolved in 100 ml of 0.2 M trifluoroacetic acid and heated at 80 °C for 4 h. The reaction was neutralized to pH 6–7 with 10% aqueous ammonia, desalted on a Sephadex G-10 column (3 × 20 cm), and passed through a small Q-Sepharose fast flow column (1 × 12 cm). The non-binding material, referred to as P-oligo, was further separated on a Sephadex G-50 column (3 × 90 cm) and eluted at 0.5 ml/min with 0.15 M NaCl. The eluate was collected at 3 ml/tube and pooled as shown in supplemental Fig. S1b.

Cell Cultures

HT-29 (human colon cancer cell line), MDA-MB-231 (human breast cancer cell line), and Jurkat (human T-lymphocyte line) cells were obtained from American Type Culture Collection. HT-29 cells were cultured in DMEM/F-12 (Invitrogen) supplemented with 10% heat-inactivated fetal calf serum (FCS), 1% penicillin, and 1% streptomycin. MDA-MB-231 cells were cultured in DMEM (Invitrogen) containing 4.5 g/liter glucose. Cell cultures were maintained at 37 °C in a humidified atmosphere of 5% CO_2 and 95% air.

Galectin-3-mediated Hemagglutination (G3H) Assay

The assay was performed as we described previously (31). Each well of a microtiter V plate contained 25 μl of 1% bovine serum albumin (BSA) in 0.15 M NaCl, 25 μl of 0.15 M NaCl (control) or the test samples in this solution, 25 μl of 12.5 μg/ml galectin-3, and 25 μl of a 4% (v/v) chicken erythrocyte suspension. Agglutination proceeded for 90 min at room temperature. The minimum inhibitory concentration (MIC) of each test sample was determined by examining a series of dilutions. The results were the average of three independent experiments.

Galectin-3-mediated Cell Adhesion Assay

HT-29 cells (7×10^4) in serum-free medium were added to each well of a 96-well plate, which was coated with galectin-3 or BSA (as background). Plates were incubated at 37 °C for 1 h in the presence or absence of the test samples. Adherent cells were measured by the 3-(4,5-dimethylthiazol-2-yl)-2,5-diphenyltetrazolium bromide method (39). Each experiment was performed in triplicate and repeated at least three times. The half-inhibitory concentration (IC_{50}) for galectin-3-mediated cell adhesion, which was determined from the absorbance at 570 nm, was obtained for each test sample by creating a dose-response curve with a nonlinear regression model in GraphPad Prism 5.0.

Asialofetuin-induced Homotypic Cell Aggregation Assay

MDA-MB-231 cells (0.6×10^6 cells/ml in PBS) were mixed with buffer (control) or 15 μg/ml ASF in the absence or presence of test samples in a 2-ml microcentrifuge tube and agitated for 1 h at 37 °C. Cell aggregation was examined under a microscope and quantified as described previously (40). Each experiment was performed in triplicate and repeated three times.

Enzyme-linked Immunosorbent Assay (ELISA)

RG-I-4 and modified RG-I-4 were coated onto 96-well Nunc Immuno MaxiSorp microtiter plates at 4 °C. The β1,4-galactan epitope was identified with monoclonal antibody LM5 according to a published method (41). Each experiment was repeated at least three times.

Fluorescent Labeling of RG-I-4 and Galectin-3

RG-I-4 and galectin-3 were labeled with DTAF according to a published method (30). Free DTAF was removed on a Sephadex G-25 column.

Fluorescence Microscopy

GST-galectin-3- and GST-immobilized beads were prepared by incubating 1 ml of glutathione-Sepharose 4B beads (GE Healthcare) with either 20 mg of GST-galectin-3 or 10 mg of GST at 4 °C for 4 h followed by extensive washing with PBS to remove unbound protein. An aliquot of the beads (5 μl) was incubated with 50 μl of 100 μg/ml DTAF-RG-I-4 at room temperature for 1 h with agitation and then washed five times with PBS or PBS containing 200 mM lactose. The beads were transferred to glass microscope slides and viewed under an epifluorescence microscope (Olympus BX 51).

Flow Cytometry Assay

One hundred microliters of Jurkat cells (10×10^6 cells/ml PBS) were incubated with 75 μg/ml (*i.e.* 2.5 μM) DTAF-galectin-3 in the absence or presence of 5 mg/ml lactose or RG-I-4 for 1 h at 25 °C. After three washes with PBS, cells were measured on a FACScan flow cytometer (BD Biosciences). The results were representative of three independent experiments.

Surface Plasmon Resonance (SPR) Assay

The affinity of pectin for galectin-3 was measured with a BIAcore T100 instrument (GE Healthcare). Galectin-3 was coupled to an activated CM5 sensor chip by injecting 50 μg/ml galectin-3, which was dissolved in 10 mM sodium acetate (pH 5.0), until an immobilized level of 8000 resonance units was obtained. The remaining active sites were blocked by injecting 1 M ethanolamine (pH 8.5). To determine the binding specificity, 0.3 mg/ml RG-I-4 or 1.65 mg/ml RG-I-4-RG was injected at 30 μl/min for 90 s followed by PBS, 150 mM lactose, and a final injection of PBS. To determine the binding kinetics, five concentrations of each pectic sample (0.313, 0.625, 1.25, 2.5, and 5.0 μM for RG-I-4 and potato galactan and 5, 10, 20, 40, and 80 μM for MCP) were injected individually at a flow rate of 30 μl/min with a single cycle kinetics program. Each concentration was injected for 90 s. Regeneration was performed with 150 mM lactose in PBS after all five concentrations had been injected. The control was obtained by injecting the same analyte solution on another channel that was immobilized with BSA. Data were analyzed with Biacore T100 evaluation software 2.0.1.

Other Analytical Methods

Sugar composition and methylation analyses were carried out according to methods that were described previously (32,

TABLE 1

The inhibitory activities of ginseng pectins on galectin-3-mediated hemagglutination

Galectin-3-mediated hemagglutination was performed in the presence or absence of each test sample. The MIC for each sample is expressed as the mean ± S.D.

Samples	MIC
	μg/ml
From ginseng	
WGPA-1-HG	45 ± 3.0
WGPA-2-HG	131 ± 5.1
WGPA-3-HG	141 ± 5.0
WGPA-4-HG	323 ± 13.9
WGPA-1-RG	91 ± 3.8
WGPA-2-RG	175 ± 9.0
WGPA-3-RG	227 ± 13.9
WGPA-4-RG	227 ± 10.2
RG-I-2	60 ± 3.8
RG-I-3B	120 ± 6.3
RG-I-4	0.25 ± 0.02
From commercial supplier	
Glucose	8000[a]
Mannose	8000[a]
Galactose	126 ± 2.6
Lactose	10 ± 1.3
Potato galactan	9.0 ± 1.1
Potato RG-I	181 ± 6.3
Larch wood AG	181 ± 6.3
MCP	0.60 ± 0.05

[a] Glucose and mannose did not show inhibition at concentrations up to 8000 μg/ml.

34). One-dimensional ^{13}C nuclear magnetic resonance (NMR) and ^{1}H NMR spectra were obtained with a Bruker AV600 spectrometer (Germany) as described previously (32, 34, 42). Two-dimensional correlation spectroscopy was recorded with a Bruker AV600 spectrometer at 298 K and 600 MHz with a spectral width of 3.15 KHz in two dimensions. High performance liquid chromatography (HPLC) was performed with a Shimadzu 10Avp HPLC system with the following columns: TSK-gel G3000PW$_{XL}$ (7.8 × 300 mm; Tosoh Corp.) eluted with 0.2 M NaCl at 0.5 ml/min, Sugar-PacK (6.5 × 300 mm; Waters) eluted with 1 mM calcium-EDTA at 0.6 ml/min at 90 °C, and Superose 6 10/300 GL (Amersham Biosciences) eluted with 0.15 M NaCl at 0.5 ml/min. Elution was monitored with a refractive index detector (RID-10A).

RESULTS

Preparation and Structural Analysis of Pectic Samples

Ginseng Pectic Samples—The ginseng pectin fractions and RG-I fragments that were prepared according to our published protocols (32–34) were the HG domain-rich fractions (WGPA-1-HG, -2-HG, -3-HG, and -4-HG), the RG-I domain-containing and AG-rich fractions (WGPA-1-RG, -2-RG, -3-RG, and -4-RG), and the RG-I fragments (RG-I-2, RG-I-3B, and RG-I-4) (Table 1).

The Structural Features of RG-I-4—As mentioned in our previous report (34), RG-I-4 is a 60-kDa RG-I domain-rich fragment that is composed mainly of GalA (33.8%), Rha (21.8%), Gal (19.5%), and Ara (9.2%) residues. GalA and Rha constitute the RG-I backbones, and Ara and Gal constitute the α1,5-arabinan and β1,4-galactan/arabino-β1,4-galactan (*i.e.* AG-I-type) side chains. The backbone in RG-I-4 has a high branching frequency of 0.67; *i.e.* there are two side chains for every three disaccharide (α1,2-Rha-α1,4-GalA-) units.

In this study, we isolated the backbone of RG-I-4, referred to as RG-I-4-RG, by removing its side chains with partial acid hydrolysis. Sugar composition analysis showed that RG-I-4-RG consisted mainly of Rha (44%) and GalA (49%) with trace amounts of Gal (4.2%), Ara (1.5%), and GlcA (0.5%). The ^{13}C NMR spectrum (Fig. 1) clearly displayed signals for α1,4-GalA (C-1 at 99.7 ppm and C-6 at 175.5 ppm) and α1,2-Rha (C-1 at 98.7 ppm and C-6 at 18.2 ppm). The ratio of the C-1 signal intensity of Rha to GalA was ~1:1. There were no signals for Ara and very weak signals for Gal (105.9, 104.9, 62.0, and 61.4 ppm). These data indicated that RG-I-4-RG was composed of a repeating disaccharide (α1,2-Rha-α1,4-GalA-), which is a typical RG-I-type structure.

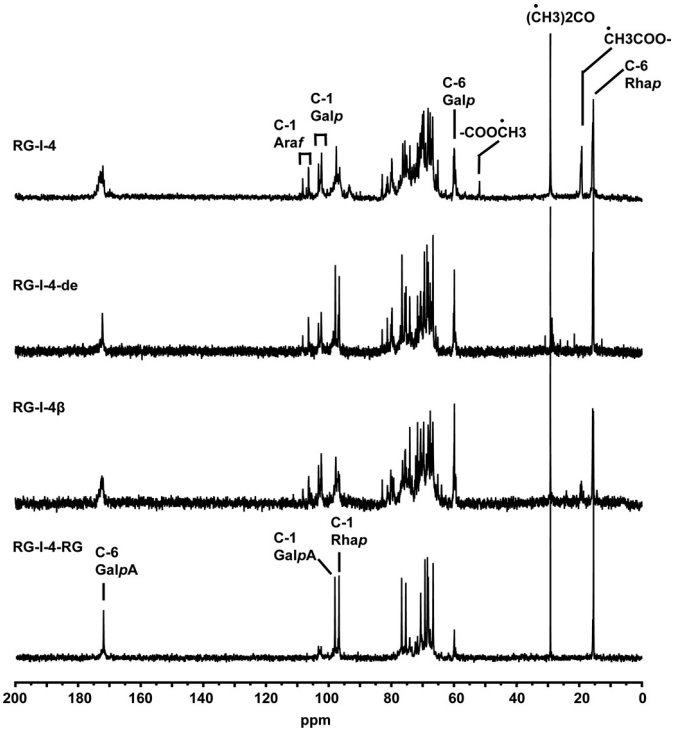

FIGURE 1. **^{13}C NMR spectra of RG-I-4 and modified RG-I-4.**

We further characterized the galactan portion of the side chains as galactan from other sources has been shown to bind galectin-3 (30, 31). Methylation analysis showed that Gal residues were mainly terminal or 1,4-linkages at a 3:2 ratio, which is consistent with ^{13}C NMR results that RG-I-4 mainly contains β1,4-galactan side chains (34). The high ratio of terminal to 1,4-linked Gal suggested that the side chains of RG-I-4 might be short with some side chains containing only 1 Gal residue. This is in line with our previous estimation of 1.87 residues per chain (34). To evaluate the chain length, we used an antibody, LM5, which recognizes β1,4-galactan chains with at least four consecutive Gal residues (41). In this study, we classified β1,4-galactan side chains that contain ≥4 consecutive Gal residues as long chains and those containing ≤3 consecutive Gal residues as short chains. Intact RG-I-4 was recognized by LM5, indicating the presence of long side chains (Table 2, RG-I-4-con). When 5% of Gal residues were removed by endo-β1,4-D-galactanase, recognition of RG-I-4 by LM5 was reduced to 50% of the control (Table 2, RG-I-4-endo-g). When 20% of the Gal residues were removed by β-galactosidase, recognition of RG-I-4 by LM5 was completely lost (Table 2, RG-I-4-exo-g). These

TABLE 2
The activities of modified RG-I-4
RG-I-4 was modified by various methods and examined with the G3H assay. The sugar compositions and responses to antibody LM5 were determined for some of the modified forms. —, not determined.

Sample	Treatment	Sugar content[a]		Response to LM5[b]	MIC	-Fold activity[c]
		Gal	Ara			
					μg/ml	
RG-I-4-con	Control	100	100	100	0.25 ± 0.02	1
RG-I-4-endo-a	Digestion (endo-α1,5-L-arabinanase)	106	73	—	0.035 ± 0.004	↑ 7.5
RG-I-4-exo-a	Digestion (α-L-arabinofuranosidase)	109	44	—	0.50 ± 0.03	↓ 2
RG-I-4-endo-g	Digestion (endo-β1,4-D-galactanase)	95	93	50	2.4 ± 0.2	↓ 9.3
RG-I-4-exo-g	Digestion (β-D-galactosidase)	80	51	0	9.4 ± 0.5	↓ 37.5
RG-I-4-de	De-esterification	—	—	—	12.5 ± 1.0	↓ 50
RG-I-4β	β-Elimination	—	—	—	2000 ± 86	↓ 8000
RG-I-4-RG	Partial hydrolysis	—	—	—	40 ± 3.8	↓ 160

[a] The contents of Gal and Ara are shown relative to the control, which was set as 100.
[b] Antibody response was determined by ELISA and is shown relative to the control, which was set as 100.
[c] The -fold activity is shown relative to the control, which was set as 1. ↑, increased; ↓, decreased.

data clearly demonstrate the correlation between removal of Gal residues and loss of antibody recognition. Furthermore, our results suggest that less than 20% of Gal residues are linked in long chains. Endo-β1,4-D-galactanase, which has a long chain substrate (β1,4-galactan), removed only a small percentage (5%) of Gal residues in RG-I-4 (Table 2, RG-I-4-endo-g), supporting the concept that most of the Gal residues are in short chains. However, under the same conditions, potato galactan, which contains long chains, was extensively hydrolyzed into oligosaccharides (supplemental Fig. S1a). Collectively, our previous data and the data presented here predict the structure for RG-I-4 shown in Fig. 2.

Galacto-oligosaccharides—Galacto-oligosaccharides were prepared from potato galactan, which contains mainly β1,4-galactan (30). Oligosaccharides A–E were prepared via enzymatic digestion (supplemental Fig. S1a), and oligosaccharides F–M were obtained by partial acid hydrolysis (supplemental Fig. S1b). Oligosaccharides A–D were eluted as single and symmetrical peaks on a Sugar-PacK column at the positions of monomer, dimer, trimer, and tetramer, respectively (Fig. 3*a*). Structural analysis by ^{1}H NMR and two-dimensional ^{1}H NMR spectra (supplemental Figs. S2 and S3) confirmed that oligosaccharides A–D were Gal, Galβ1,4-Gal, Galβ1,4-Galβ1,4-Gal, and Galβ1,4-Galβ1,4-Galβ1,4-Gal, respectively. The assignment of each signal is listed in supplemental Table S1. Oligo E was a mixture with an average molecular mass of 1 kDa, which was equivalent to 6.1 sugar residues (6.1-mer) (Fig. 3*b*). Enzymatic digestion gave rise to few oligosaccharides that were longer than a tetramer. Longer oligosaccharides were prepared by partial acid hydrolysis. After removing the acidic portion with an anion exchange column, the neutral oligosaccharide portion, referred to as P-oligo, was obtained. P-oligo was composed of 96.7% Gal and 3.3% Ara residues and displayed a broad peak on a TSK-gel G3000 column (Fig. 3*b*). Linkage analysis by methylation showed that almost all of the Gal residues were in the form of 1,4- and terminal linkages, indicating that P-oligo consists of linear β1,4-galacto-oligosaccharides. The subfractions, oligosaccharides F–M, had similar sugar compositions and displayed narrower peaks on the TSK-gel G3000 column (Fig. 3*b*). Their molecular masses ranged from 1.2 (oligosaccharide F) to 10.6 kDa (oligosaccharide M), which was equivalent to 7.3–65.3 Gal residues per oligosaccharide.

RG-I-4, a Ginseng Pectic Domain, Was a Potent Inhibitor in the G3H Assay

The G3H assay is widely used for evaluating potential galectin-3 inhibitors by measuring the MIC of sample for galectin-3-mediated hemagglutination (19). All ginseng pectins prepared from the native ginseng polysaccharides and the RG-I fragments prepared from endo-PG-digested ginseng pectin were examined (Table 1). Among the intact ginseng pectins, WGPA-1-HG exhibited the strongest inhibition of G3H with an MIC of 45 ± 3.0 μg/ml followed by WGPA-1-RG, which had an MIC of 91 ± 3.8 μg/ml. The weakest ginseng pectin was WGPA-4-HG, which had an MIC of 323 ± 13.9 μg/ml. In comparison, lactose, a standard galectin-3 inhibitor, showed an MIC of 10 ± 1.3 μg/ml. These results indicated that all intact ginseng pectins including HG-rich and AG-rich pectins could inhibit galectin-3 but in a relatively weak manner. Among the RG-I-rich fragments, the MICs of RG-I-2 and RG-I-3B were 60 ± 3.8 and 120 ± 6.3 μg/ml, respectively, similar to the intact ginseng pectins and the commercially purchased potato RG-I fragments (MIC = 181 ± 6.3 μg/ml) and larch wood AG (MIC = 181 ± 6.3 μg/ml). In contrast, the MIC of RG-I-4 was 0.25 ± 0.02 μg/ml, which was significantly lower than other ginseng pectins. In fact, it was the lowest among all of the pectic samples examined including MCP (MIC = 0.6 ± 0.05 μg/ml) and potato galactan (MIC = 9.0 ± 1.1 μg/ml), which are two well established galectin-3 ligands. Thus, we identified an RG-I-rich fragment that is a potent inhibitor of galectin-3.

RG-I-4 Inhibited Galectin-3-mediated Cell Adhesion

RG-I-4-mediated inhibition of galectin-3 was further investigated at the cellular level. Galectin-3-mediated cell adhesion plays an important role in cancer progression and metastasis. Here, the effect of RG-I-4 on galectin-3-mediated HT-29 cell adhesion was examined and compared with that of lactose,

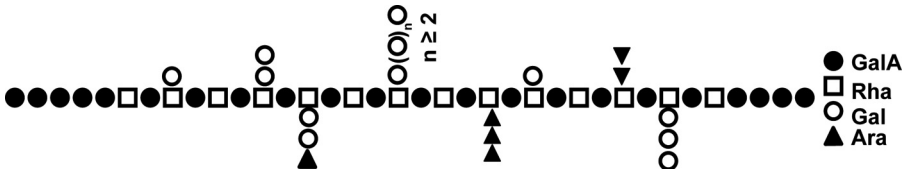

FIGURE 2. **The structure diagram of RG-I-4.**

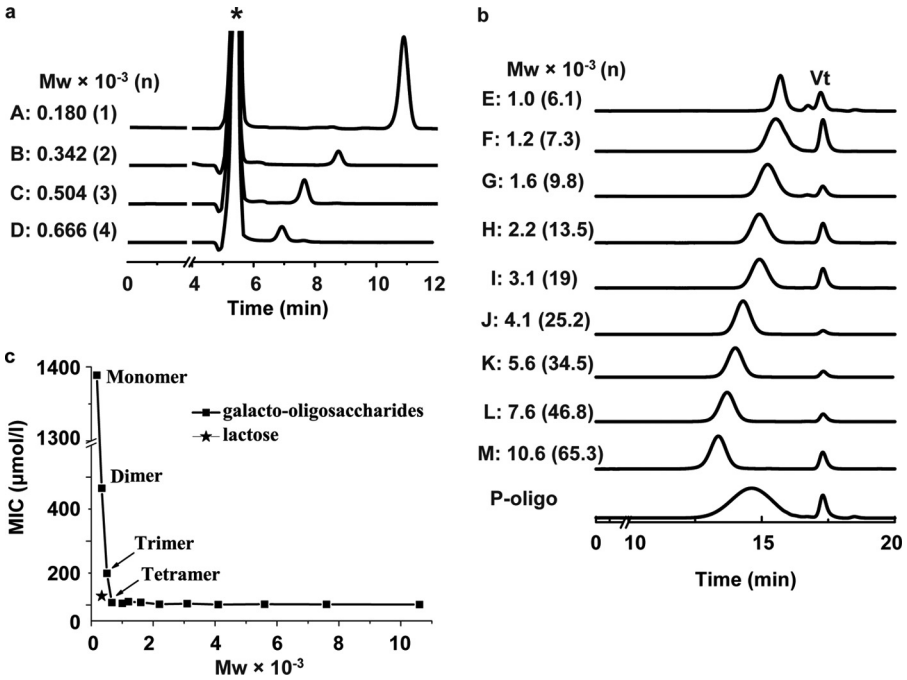

FIGURE 3. **The molecular weights and activities of the galacto-oligosaccharides.** *a*, the elution profiles of oligosaccharides A–D on a Sugar-PacK column. *b*, the elution profiles of oligosaccharides E–M on a TSK-gel G3000 column. The molecular weight and corresponding number of sugar residues (*n*) is presented next to the name of each oligosaccharide. *c*, correlation between the activity and length of oligosaccharides. The activity was determined by the G3H assay. *, PBS; *Vt*, total volume of the column.

potato galactan, and MCP. As expected, lactose inhibited galectin-3-mediated cell adhesion (Fig. 4*a*) with an IC_{50} of 5.1 μg/ml. Potato galactan showed a similar effect with an IC_{50} of 10.3 μg/ml (Fig. 4*b*). MCP exerted stronger inhibition than both lactose and potato galactan with an IC_{50} of 0.3 μg/ml (Fig. 4*c*). Remarkably, RG-I-4 showed 15-fold stronger inhibition than MCP with an IC_{50} of 0.02 μg/ml (Fig. 4*d*). In contrast, sucrose did not inhibit galectin-3-mediated cell adhesion at concentrations up to 800 μg/ml (data not shown). The inhibition exerted by these samples was in an order similar to that observed in the G3H assay, which suggests that RG-I-4 is a potent inhibitor of galectin-3.

RG-I-4 Inhibited Galectin-3-related Cancer Cell Aggregation

Homotypic cell aggregation in the blood stream contributes to tumor cell embolization and is associated with increased metastasis (11, 43). MCP has been shown to inhibit ASF-induced cell aggregation by disrupting interactions between galectin-3 on the cell surface and glycol ligands on ASF (18, 40). We examined whether RG-I-4 inhibits ASF-induced cell aggregation (Fig. 5*a*). The inhibitory activity of RG-I-4 was compared with lactose, potato galactan, MCP, and sucrose. As shown in Fig. 5*b*, all of the tested samples except sucrose (data not shown) showed inhibitory effects. However, the effective doses for each compound were markedly different. Lactose and potato galactan did not inhibit aggregation until 10 μg/ml. In contrast, RG-I-4 and MCP markedly inhibited aggregation at concentrations as low as 0.05 and 0.1 μg/ml, respectively. These data indicated that RG-I-4 was a potent inhibitor of ASF-induced cell aggregation.

RG-I-4 Inhibited the Binding of Galectin-3 to T-cells

Galectin-3 binds to T-cells, resulting in inhibition of T-cell activation and induction of apoptosis. These events may contribute to the escape of tumor cells from the immune system (13). Here, we used flow cytometry to determine whether RG-I-4 inhibits binding of fluorescently labeled galectin-3 (DTAF-galectin-3) to Jurkat cells, a human T-lymphocyte line. In the absence of any inhibitors (Fig. 6*a*), a high density of DTAF-galectin-3 bound to cells as indicated by the high fluorescence intensity. In the presence of 5 mg/ml lactose (Fig. 6*b*), the fluorescence intensity decreased dramatically. In the presence of 5 mg/ml RG-I-4 (Fig. 6*c*), the fluorescence intensity was further decreased, indicating that RG-I-4 exerted stronger inhibition than lactose. Thus, RG-I-4 potently inhibited binding of galectin-3 to T-cells.

RG-I-4 Bound to the CRD of Galectin-3

To validate direct binding between RG-I-4 and galectin-3, we labeled RG-I-4 with a fluorescent dye, DTAF, and incubated

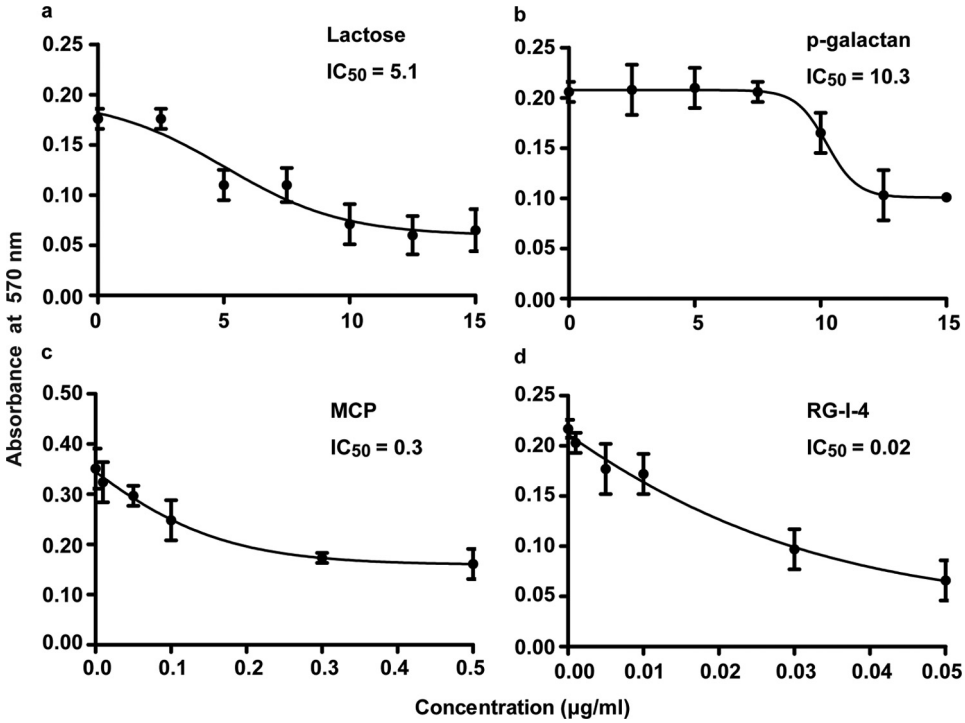

FIGURE 4. **Inhibition of galectin-3-mediated cell adhesion.** HT-29 cells were plated in wells coated with galectin-3 and incubated for 1 h in the presence of lactose (*a*), potato galactan (*p-galactan*) (*b*), MCP (*c*), and RG-I-4 (*d*). Adherent cells were measured by the 3-(4,5-dimethylthiazol-2-yl)-2,5-diphenyltetrazolium bromide assay. The IC_{50} of each sample was determined from the corresponding dose-response curve. *Error bars* represent the S.D. of triplicate measurements of at least three independent experiments.

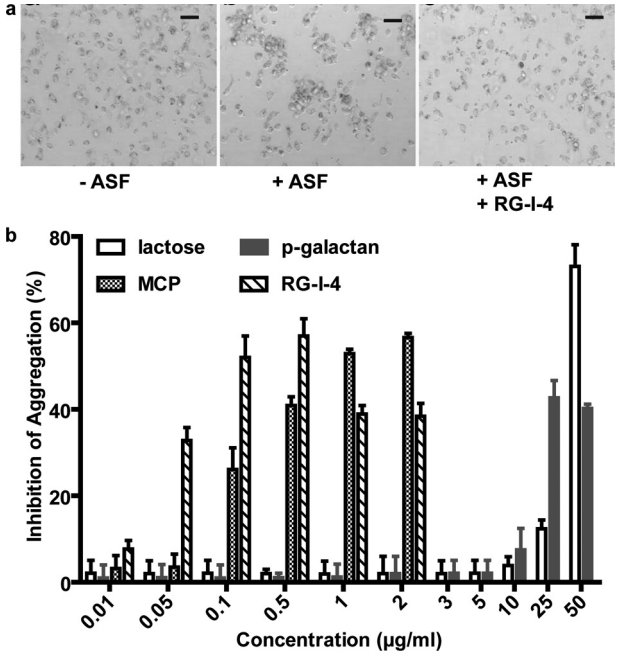

FIGURE 5. **Inhibition of ASF-induced cell aggregation.** MDA-MB-231 cells were agitated in the absence or presence of ASF supplemented with or without test samples. Cells were photographed with a phase-contrast microscope (*a*), and inhibition of aggregation was determined (*b*). *a*, representative images showing that 0.5 μg/ml RG-I-4 inhibits aggregation. *b*, quantification of inhibition of aggregation is shown for samples exposed to lactose, MCP, RG-I-4, or potato galactan (*p-galactan*). *Error bars* represent the S.D. of triplicate measurements of at least three independent experiments. *Scale bars*, 10 μm.

DTAF-RG-I-4 with galectin-3-coupled beads. After incubation, the beads were washed with PBS or 200 mM lactose and viewed under a fluorescence microscope. As shown in Fig. 7,

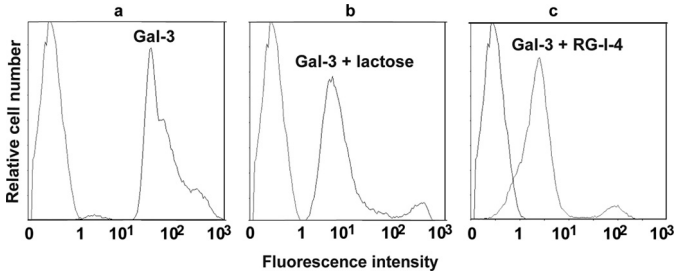

FIGURE 6. **Inhibition of galectin-3 binding to Jurkat cells.** Jurkat cells that were incubated with DTAF-galectin-3 (*Gal-3*) in the absence (*a*) or presence of 5 mg/ml lactose (*b*) or 5 mg/ml RG-I-4 (*c*) were measured by flow cytometry. Cells incubated with buffer alone were used as a control.

DTAF-RG-I-4 did not bind to the control beads (Fig. 7*a*) but bound to the beads with immobilized galectin-3 (Fig. 7*b*). Bound DTAF-RG-I-4 was completely washed off by lactose (Fig. 7*c*). These results demonstrate that RG-I-4 binds specifically to the CRD of galectin-3.

Binding of RG-I-4 to galectin-3 was examined further by SPR analysis with a Biacore T100 instrument. Galectin-3 was immobilized on a CM5 sensor chip, and RG-I-4 in PBS was allowed to flow over the chip. As shown in Fig. 8*a*, the response increased by ~150 resonance units after injection of 0.3 mg/ml RG-I-4 for 90 s (*arrow A*). The response remained largely unchanged when PBS was injected (*arrow B*), indicating that RG-I-4 was tightly associated with galectin-3. After the injection of 150 mM lactose (*arrow C*) followed by PBS (*arrow D*), the response returned to base line, indicating that RG-I-4 was completely washed off by lactose. This provided further evidence that binding of RG-I-4 was dependent on the CRD of galectin-3.

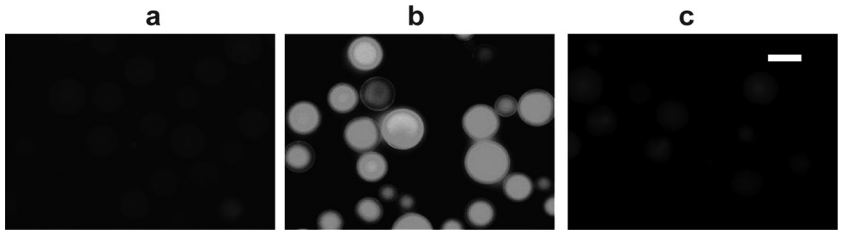

FIGURE 7. **Binding of RG-I-4 to immobilized galectin-3.** DTAF-RG-I-4 was incubated with GST- (*a*) or GST-galectin-3-immobilized beads (*b* and *c*) and subsequently washed with PBS (*a* and *b*) or PBS plus 200 mM lactose (*c*). The cells were viewed and photographed at 400× *magnification*. *Scale bar*, 100 μm.

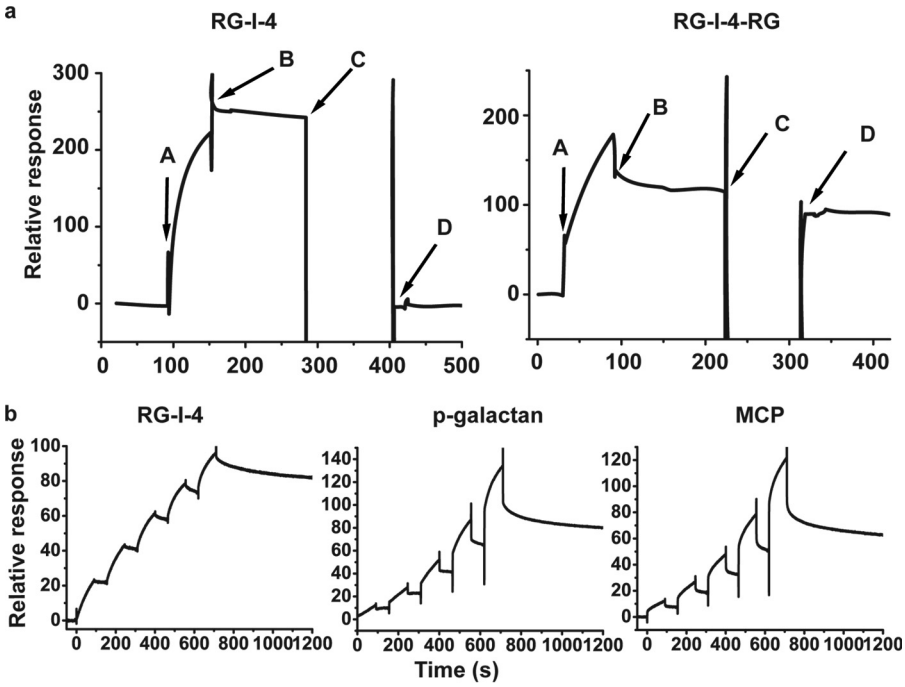

c

Samples	ka (1/Ms)	kd (1/s)	K_D (nM)	K_D (μg/ml)
RG-I-4	6530	1.447×10^{-4}	22.2	1.33
MCP	163.8	4.243×10^{-4}	2590	61.5
p-galactan	2397	3.418×10^{-4}	143	38.9

FIGURE 8. **SPR analysis of the binding affinities of pectins to galectin-3.** *a*, the sensorgrams of RG-I-4 and RG-I-4-RG. The samples were injected at 30 μl/min (*arrow A*) for 90 s followed by PBS (*arrow B*), 150 mM lactose (*arrow C*), and finally PBS (*arrow D*). *b*, the binding kinetics of RG-I-4, potato galactan (*p-galactan*), and MCP. Five concentration gradients of each sample were injected with a single cycle kinetics program. The injection lasted for 90 s for each concentration. *c*, the binding kinetic parameters. The data shown in *b* were analyzed with Biacore T100 evaluation software 2.0.1 according to a 1:1 binding model.

RG-I-4 Bound Galectin-3 with High Affinity

The binding kinetics of RG-I-4 with galectin-3 were determined by SPR and compared with those of MCP and potato galactan. Five concentrations were tested for each pectic polysaccharide with a "single cycle kinetics" program and analyzed with Biacore T100 evaluation software 2.0.1 (Fig. 8, *b* and *c*). The dissociation constants (K_D) derived from the association and dissociation rate constants were 22.2 nM for RG-I-4 (*i.e.* 1.33 μg/ml based on its molecular mass of 60 kDa), 2590 nM for potato galactan (*i.e.* 38.9 μg/ml based on its molecular mass of 272 kDa), and 143 nM for MCP (*i.e.* 61.5 μg/ml based on its molecular mass of 30 kDa). These data indicate that the binding affinity of RG-I-4 for galectin-3 was significantly higher than that of MCP and potato galactan, which is consistent with our data showing potent inhibition of galectin-3-mediated effects by RG-I-4.

Ara Residues Regulate the Activity of RG-I-4

According to our previous work, Ara residues in RG-I-4 exist as 5-substituted or terminal residues within the α1,5-arabinan/AG-I side chains (34). To study the roles played by Ara, we treated RG-I-4 with endo-α1,5-L-arabinanase or α-L-arabinofuranosidase, yielding RG-I-4-endo-a and RG-I-4-exo-a, respectively. In comparison with buffer-treated RG-I-4 (RG-I-4-

TABLE 3
Comparison of the structures of RG-I-2, RG-I-3B, and RG-I-4

Pectin	Sugar composition[a]				Molecular mass[a]	No. of total sugar[b]	No. of total Rha[c]	Branch/total Rha[d]	No. of branch Rha[e]
	GalA	Rha	Gal	Ara					
	mol %				*kDa*				
RG-I-2	44.3	11.7	12.4	14.5	4	25	2.9	0.51	1.5
RG-I-3B	44.6	14.1	13.7	11.9	6	38	5.4	0.75	4.0
RG-I-4	33.8	21.8	19.5	9.2	60	375	81.8	0.67	55

[a] Data quoted from Ref. 34.
[b] The estimated number of total sugar residues in a molecule = Molecular weight ÷ 160, an average molecular weight of a sugar residue.
[c] The number of total Rha in a molecule = Rha content × Number of total sugar residues.
[d] The ratio of branching to total Rha quoted from Table 3 (in the name of A/B) in Ref. 34.
[e] The number of branching Rha in a molecule = Number of total Rha × Ratio of branching to total Rha.

con), Ara content in RG-I-4-endo-a and RG-I-4-exo-a was decreased by 27 and 56% (Table 2), respectively. Endo-α1,5-L-arabinanase treatment increased the G3H activity of RG-I-4 by 7.5-fold (Table 2, RG-I-4-endo-a) in comparison with the control, suggesting that α1,5-L-arabinan chains are not required but may restrict the activity of RG-I-4. In contrast, α-L-arabinofuranosidase, which cleaves the terminal Ara residues in both α1,5-L-arabinan and AG-I chains, decreased the G3H activity of RG-I-4 by 2-fold (Table 2, RG-I-4-exo-a). Together, these data indicate that Ara residues can positively or negatively regulate the activity of RG-I-4 depending on their locations. The α1,5-L-arabinan side chains impaired the activity, whereas the terminal Ara residues in the AG-I side chains promoted the G3H activity of RG-I-4.

β1,4-Galactan Side Chains Played Important Roles in the Activity of RG-I-4

To study the roles played by Gal residues, we treated RG-I-4 with either β-galactosidase or endo-β1,4-D-galactanase, yielding RG-I-4-exo-g and RG-I-4-endo-g, respectively. In comparison with the control, the Gal content in RG-I-4-exo-g and RG-I-4-endo-g was reduced by 20 and 5%, respectively (Table 2). The activities of RG-I-4-exo-g and RG-I-4-endo-g in the G3H assay were decreased by 37.5- and 9.3-fold (Table 2), respectively, indicative of the important roles played by Gal residues. Because Gal residues in RG-I-4 are mainly located in the β1,4-galactan side chains, we concluded that these side chains are the functional structural elements.

The Contributions of the Length of β1,4-Galactan Side Chains to the Activity of RG-I-4

Structural analysis indicated that RG-I-4 contained mainly short chains of ≤3 Gal residues and only a small percentage of side chains with ≥4 Gal residues. When the long chains were partially removed, the activity decreased by 9.3-fold (Table 2) as in the case of RG-I-4-endo-g, which exhibited a 50% reduction in antibody recognition. When the long chains were completely removed, the activity decreased by 37.5-fold (Table 2) as in the case of RG-I-4-exo-g, which lost antibody recognition. These data demonstrate the important contributions that long chains make to RG-I-4 activities. However, even when the long chains were completely removed as in the case of RG-I-4-exo-g, activity still remained relatively high (MIC of 9.4 ± 0.5 μg/ml) and was equivalent to the activity of potato galactan (MIC of 9.0 ± 1.1 μg/ml). Thus, the short chains also contribute significantly to RG-I-4 activity.

To understand the correlation between chain length and activity, we prepared a series of β1,4-galacto-oligosaccharides from potato galactan and examined their activities in the G3H assay (Fig. 3*c*). The MIC decreased significantly for the tetramer *versus* monomer and changed little thereafter (Fig. 3*c*). The MIC of the tetramer was slightly lower than lactose (Fig. 3*c*, *asterisk*). These data indicate that oligosaccharides that were longer than or equivalent to a tetramer had similar activities that were slightly better than lactose. The oligosaccharides that were shorter than a tetramer had 13- (trimer), 48.7- (dimer), and 185-fold (monomer) lower activities than lactose. These data suggest that a chain of 4 Gal residues meets the basic need for maximum activity. Based on these data, we deduce that a long side chain (greater than or equal to a tetramer) in RG-I-4 has slightly better activity than lactose, whereas a short chain (less than or equal to a trimer) has lower activity than lactose.

Multiple β1,4-Galactan Chains Determined the High Activity of RG-I-4

As shown above, the functional elements of RG-I-4 were β1,4-galactan side chains. However, RG-I-4 had 40–1000-fold higher activity than a single β1,4-galactan chain. Why did RG-I-4 have such high activity? Structural analysis showed that an RG-I-4 molecule has 55 side chains, a feature distinct from other ginseng RG-I samples of low activity (*e.g.* RG-I-2 had 1.5 side chains, and RG-I-3B had 4 side chains; Table 3). To determine whether this feature is related to the extraordinary activity, we fragmented RG-I-4 by β-elimination, which cleaves pectic polysaccharides at the methyl-esterified GalA residues on the backbone (38). We hypothesized that if the cooperative action of the side chains contributes to the activity of RG-I-4 then fragments with fewer side chains would have much lower activity. As shown in Fig. 9, RG-I-4 was cleaved into fragments, which are referred to as RG-I-4β. Each RG-I-4β fragment has an estimated molecular mass of 11 kDa and about 10 side chains. The ^{13}C NMR spectrum of RG-I-4β was similar to that of RG-I-4 except for slight differences corresponding to the GalA and Rha residues (Fig. 1). These data indicate that β-elimination occurred only on some GalA residues and did not alter the side chains as reported previously (38). The G3H assay showed that the activity of RG-I-4β was decreased by 8000-fold in comparison with untreated RG-I-4 (Table 2). Clearly, the number of side chains played a major role in the activity of RG-I-4. Based on the predicted molecular mass of 11 kDa, the MIC of RG-I-4β (2000 μg/ml) was calculated to be 180 μM, which is between the MIC of the dimer (366 μM) and trimer (99

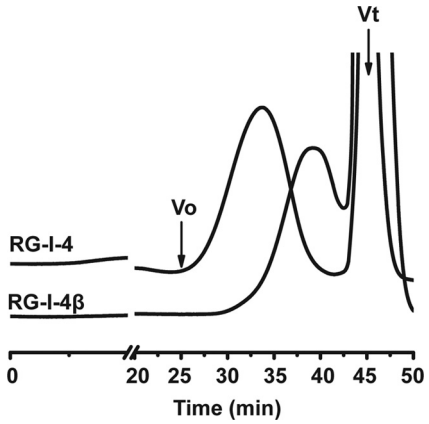

FIGURE 9. **The elution profiles of RG-I-4 and RG-I-4β on Superose 6 column.** *Vt*, total volume of the column; *Vo*, void volume.

μM). This result is consistent with our conclusion that the majority of side chains in RG-I-4 are short.

The Backbone of RG-I-4 Regulated Its Activity

Two common modifications that occur naturally to the GalA residues of the RG-I backbone are methyl esterification and acetylation. Because these modifications were shown to often affect the activities of other pectins, we investigated whether they affect the activity of RG-I-4. We de-esterified RG-I-4 (RG-I-4-de) according to the published method (32). This treatment successfully removed methyl and acetyl groups as indicated by the disappearance of ^{13}C NMR signals at 53.4 ppm, which represents the methyl carbon of the methyl ester groups of GalA, and 22.0 ppm, which represents the methyl carbon of the acetyl groups in O-2 or O-3 of GalA (Fig. 1). The G3H assay showed that the inhibitory activity of the de-esterified RG-I-4 was decreased by 50-fold in comparison with untreated RG-I-4 (Table 2). This experiment provided further evidence that the backbone of RG-I-4 plays important roles.

The Isolated Backbone of RG-I-4 Bound Galectin-3 in a CRD-independent Manner

Next, we isolated the backbone of RG-I-4, which is referred to as RG-I-4-RG, and investigated whether it interacts with galectin-3. We speculated that RG-I-4-RG would not have anti-galectin-3 activity as it contained very few Gal residues. To our surprise, RG-I-4-RG inhibited activity in the G3H assay, although higher concentrations were required relative to intact RG-I-4 (Table 2). To understand its activity further, we measured interaction of RG-I-4-RG with galectin-3 by SPR. As shown in Fig. 8*a*, the response increased by ~100 resonance units after injection of 1.65 mg/ml RG-I-4-RG for 90 s (*arrow A*). The response dropped slightly when PBS was injected (*arrow B*), indicating that RG-I-4-RG was tightly associated with galectin-3. However, bound RG-I-4-RG could not be washed off by 150 mM lactose (*arrow C*), indicating that binding was independent of the CRD of galectin-3 (*i.e.* the binding was nonspecific). We questioned whether this nonspecific interaction facilitates binding of the whole RG-I-4 molecule to galectin-3. Based on the fact that the bond between galectin-3 and RG-I-4 could be completely broken by lactose (Fig. 8*a*), we concluded that binding between galectin-3 and RG-I-4 did not involve nonspecific interactions.

DISCUSSION

Inhibitors of galectin-3 that are derived from edible natural products are of important value because of their low toxicities. Pectin-derived inhibitors have been shown to inhibit various galectin-3-mediated events during tumor development and metastasis (18–24, 27, 28). However, the structural elements of pectin that mediate inhibition of galectin-3 are poorly defined. In this study, we address this issue using a series of ginseng pectins and fragments that were prepared and characterized by our group (32–34).

The Inhibitory Activities and Binding Properties of RG-I-4 to Galectin-3

All of the fractions that were isolated from intact ginseng pectin were evaluated for their abilities to inhibit galectin-3 by the G3H assay. All of the fractions exhibited weak inhibition with MIC values ranging from 45 to 323 μg/ml, although the Gal contents ranged from 3.5 to 56.2% (32, 33). These results suggested that the activity of the pectin was not solely determined by its Gal content. Subsequently, we examined RG-I fragments isolated from endo-PG-treated ginseng pectin and found that one of the RG-I fragments, RG-I-4, strongly inhibited galectin-3-mediated hemagglutination. Its effect was 40 times stronger than lactose and stronger than all reported inhibitors derived from pectic sources. RG-I-4 also inhibited galectin-3-mediated cell adhesion, homotypic cell aggregation, and galectin-3 binding to T-cells.

Binding of RG-I-4 to galectin-3 was investigated using microscopy and SPR. Both methods demonstrated that RG-I-4 specifically bound to the CRD of galectin-3. The affinity of RG-I-4 for galectin-3 was higher than for other pectic polysaccharides, consistent with its high inhibitory activity of galectin-3.

It is interesting that intact ginseng pectin has low activity, whereas modification (endo-PG digestion in this case) generated highly active components such as RG-I-4. This phenomenon was also observed in the case of citrus pectin, which is activated by pH modification, although the parental material is inactive. The active elements might be concealed in the parental material by other sugars, linkages, or the overall conformation of the molecules.

Correlation of the Structure and Activity of RG-I-4

The Effects of the Side Chains of RG-I-4 on Binding to Galectin-3—The results of the G3H assay showed that hydrolyzing Ara residues either slightly impaired or enhanced the activity depending on the location of the residues. Thus, Ara residues regulate RG-I-4 activity. In contrast, hydrolysis of Gal residues markedly decreased RG-I-4 activity, suggesting that Gal residues play a pivotal role. Because Gal residues in RG-I-4 are located in the galactan side chains, we concluded that these side chains are the functional structural elements. This is consistent with previous reports that showed that galactans from potato pectin (30) and MCP (31) interact with galectin-3.

It has been reported that potato galactan consists of long β1,4-galactan chains with an average chain length of ~22 residues (30). We confirmed the presence of long chains by isolating galacto-oligosaccharides as long as 63.5 residues from potato galactan (Fig. 3*b*). MCP galactan also consists of long β1,4-galactan chains with ~110 Gal residues (18 kDa) according to our previous study (31). By analogy, we initially speculated that RG-I-4 activity is regulated by its long galactan side chains. However, structural analysis indicated that RG-I-4 contained mainly short chains of ≤3 Gal residues and only a small percentage of side chains with ≥4 Gal residues. Furthermore, when the long chains (≥4 Gal residues) were completely hydrolyzed, activity was considerably reduced but still high. Thus, although the long chains contribute to its activity, the short chains play major roles in regulating the activity of RG-I-4 in contrast to potato and MCP galactans.

The above discovery led us to further investigate the relationship between chain length and RG-I-4 activity. Because of the difficulty of isolating individual side chains in reasonable quantities, we prepared various β1,4-galacto-oligosaccharides from potato galactan. We found that the activity was significantly increased for the tetramer *versus* the monomer with only a slight change in activity for long chains up to a 63.5-mer. Based on these data, we deduced that the activity of a single chain in RG-I-4 is proportional to its length up to 4 Gal residues. Furthermore, all long chains with ≥4 Gal residues had similar activities.

It has been proposed that the CRD of galectin-3 possesses an extended binding site that can accommodate 4 sugar residues. Our data showing that the activity increased as the chain lengthened from a monomer to a tetramer of Gal residues fit well with this model. Thus, we provide experimental evidence supporting the proposed mechanisms of binding. The remaining question is whether galectin-3 recognizes the internal or terminal tetrasaccharide within a galactan chain. According to our studies on MCP galactan that showed that the activities are proportional to the number of chain termini (31), we propose that galectin-3 recognizes terminal tetrasaccharides. In the case of poly(LacNAc), galectin-3 appears to primarily recognize internal LacNAc units as stated by the authors (44).

The Cooperation of the Side Chains—It is intriguing that RG-I-4 had significantly higher activity than other galactans. Further studies demonstrated that the high activity of RG-I-4 resulted from the cooperative actions of the side chains. This conclusion is based on four lines of evidence. First, RG-I-4 is a highly branched molecule with galactan side chains, providing the opportunity for multivalent interactions. Second, an individual side chain has significantly lower activity than the whole molecule. Third, cleaving the backbone yielded fragments with fewer side chains that had significantly lower activity. Finally, modification of the backbone, which might sterically affect the orientation of the side chains, significantly decreased the activity.

How does cooperation between side chains affect the activity of pectin? In contrast to many carbohydrate-binding proteins, galectin-3 has one binding site. However, upon binding to multivalent ligands, galectin-3 forms multimers and acquires multiple binding sites (5). As a result, the avidity of a multivalent ligand for galectin-3 is dramatically increased because there are multiple binding sites on galectin-3 and its ligand. Multivalency of the ligand is more prominent in the case of galectin-3 than for other carbohydrate-binding proteins. Thus, it is not surprising that the multivalency and cooperativity of the RG-I-4 side chains become dominating factors determining pectin activity.

The mode of cooperative action explains the relatively low activity of MCP galactans (31). The activity of MCP galactans (MIC = 50 μg/ml) falls in the range of galacto-oligosaccharides. As demonstrated by our previous study, MCP galactans are linear chains (31), suggesting that they are monovalent and unable to induce multimerization of galectin-3. The lack of multivalency in both MCP galactan and galectin-3 is associated with low affinity. In the case of potato galactan, the situation is more complicated. The activity of potato galactan is similar to its long oligosaccharide derivatives. Although there are multiple side chains, they do not appear to work cooperatively. The location and/or orientation of the side chains might not be suitable for binding and inducing formation of a galectin-3 oligomer. An interesting future goal is to find out which pectin structures can induce oligomerization.

The Roles of the Backbone—The significant decrease in activity after cleavage and modification of the backbone clearly demonstrated the involvement of the backbone in the activity of the whole molecule. The backbone maintains a proper structural conformation so that the side chains can work cooperatively. Although nonspecific interaction between galectin-3 and the isolated backbone was observed, such nonspecific interaction was not observed between galectin-3 and the intact molecule. The backbone in RG-I-4 has a high branching frequency of 0.67; *i.e.* there are two side chains for every three disaccharide (α1,2-Rha-α1,4-GalA-) units (34). Such high branching frequency might completely conceal the active groups of the backbone.

How do we understand the interaction between galectin-3 and the isolated backbone? In this study, the G3H and SPR experiments were performed at pH 7.2, a physiological condition. At this pH, galectin-3 was positively charged (30), whereas the isolated backbone RG-I-4-RG, which contains 49% GalA, was negatively charged. Thus, the association between galectin-3 and the isolated backbone might be based on ionic interaction. Protein-pectin interactions based on ionic charge were observed for galectin-3 and other pectic polysaccharides such as potato RG-I and citrus homogalacturonic acid (30). However, our preliminary experiments revealed that DTAF-labeled RG-I-4-RG could not be eluted from galectin-3-immobilized beads by a high concentration of NaCl up to 4 M (data not shown). Thus, ionic interaction might not be an appropriate explanation. There might be secondary carbohydrate recognition sites within the galectin-3 molecule. Investigations to solve this issue are going on in our research group.

More Evidence Derived from Comparative Analyses of RG-I-2, RG-I-3B, and RG-I-4—RG-I-2, RG-I-3B, and RG-I-4 are RG-I-type ginseng pectins. RG-I-2 and RG-I-3B showed much weaker activity than RG-I-4. Table 3 lists the structural data for these pectins and is based on data from a previous publication (34) and from analyses in the current study. We compared the structures and found that (*a*) the content of Gal and the ratio of Gal/Ara in RG-I-4 (19.5% and 2.12, respectively) were about

twice those in RG-I-3B (13.7% and 1.15) and RG-I-2 (12.4% and 0.86). (*b*) All Gal residues in RG-I-4 resided in the AG-I-type side chains, whereas Gal residues in RG-I-2 and RG-I-3B resided in either AG-I- or AG-II-type (*i.e.* β1,3,6-D-galactan or arabino-β1,3,6-D-galactan) side chains. (*c*) 55 side chains were linked to C-4 of Rha in the RG-I-4 molecule, which was dramatically higher than RG-I-3B and RG-I-2 (4 and 1.5, respectively). These data suggest that high Gal content, the Gal/Ara ratio, the AG-I-type side chains, and the total number of side chains on the backbone play important roles. Thus, the information gained by comparing these pectins was consistent with the experimental results obtained in this study.

REFERENCES

1. Dumic, J., Dabelic, S., and Flögel, M. (2006) Galectin-3: an open-ended story. *Biochim. Biophys. Acta* **1760,** 616–635
2. Demetriou, M., Granovsky, M., Quaggin, S., and Dennis, J. W. (2001) Negative regulation of T-cell activation and autoimmunity by Mgat5 N-glycosylation. *Nature* **409,** 733–739
3. Thijssen, V. L., Poirier, F., Baum, L. G., and Griffioen, A. W. (2007) Galectins in the tumor endothelium: opportunities for combined cancer therapy. *Blood* **110,** 2819–2827
4. Seetharaman, J., Kanigsberg, A., Slaaby, R., Leffler, H., Barondes, S.H., and Rini, J.M. (1998) X-ray crystal structure of the human galectin-3 carbohydrate recognition domain at 2.1-Å resolution. *J. Biol. Chem.* **273,** 13047–13052
5. Ahmad, N., Gabius, H. J., André, S., Kaltner, H., Sabesan, S., Roy, R., Liu, B., Macaluso, F., and Brewer, C. F. (2004) Galectin-3 precipitates as a pentamer with synthetic multivalent carbohydrates and forms heterogeneous cross-linked complexes. *J. Biol. Chem.* **279,** 10841–10847
6. John, C.M., Leffler, H., Kahl-Knutsson, B., Svensson, I., and Jarvis, G.A. (2003) Truncated galectin-3 inhibits tumor growth and metastasis in orthotopic nude mouse model of human breast cancer. *Clin Cancer Res.* **9,** 2374–2383
7. Liu, F. T., and Rabinovich, G. A. (2005) Galectins as modulators of tumour progression. *Nat. Rev. Cancer* **5,** 29–41
8. Argüeso, P., Guzman-Aranguez, A., Mantelli, F., Cao, Z., Ricciuto, J., and Panjwani, N. (2009) Association of cell surface mucins with galectin-3 contributes to the ocular surface epithelial barrier. *J. Biol. Chem.* **284,** 23037–23045
9. Iurisci, I., Tinari, N., Natoli, C., Angelucci, D., Cianchetti, E., and Iacobelli, S. (2000) Concentrations of galectin-3 in the sera of normal controls and cancer patients. *Clin Cancer Res.* **6,** 1389–1393
10. Fukumori, T., Kanayama, H. O., and Raz, A. (2007) The role of galectin-3 in cancer drug resistance. *Drug Resist. Updat.* **10,** 101–108
11. Glinsky, V. V., Glinsky, G. V., Rittenhouse-Olson, K., Huflejt, M. E., Glinskii, O. V., Deutscher, S. L., and Quinn, T. P. (2001) The role of Thomsen-Friedenreich antigen in adhesion of human breast and prostate cancer cells to the endothelium. *Cancer Res.* **61,** 4851–4857
12. Nangia-Makker, P., Honjo, Y., Sarvis, R., Akahani, S., Hogan, V., Pienta, K. J., and Raz, A. (2000) Galectin-3 induces endothelial cell morphogenesis and angiogenesis. *Am. J. Pathol.* **156,** 899–909
13. Fukumori, T., Takenaka, Y., Yoshii, T., Kim, H. R., Hogan, V., Inohara, H., Kagawa, S., and Raz, A. (2003) CD29 and CD7 mediate galectin-3-induced type II T-cell apoptosis. *Cancer Res.* **63,** 8302–8311
14. Zou, J., Glinsky, V. V., Landon, L. A., Matthews, L., and Deutscher, S. L. (2005) Peptides specific to the galectin-3 carbohydrate recognition domain inhibit metastasis-associated cancer cell adhesion. *Carcinogenesis* **26,** 309–318
15. Rabinovich, G. A., Cumashi, A., Bianco, G. A., Ciavardelli, D., Iurisci, I., D'Egidio, M., Piccolo, E., Tinari, N., Nifantiev, N., and Iacobelli, S. (2006) Synthetic lactulose amines: novel class of anticancer agents that induce tumor-cell apoptosis and inhibit galectin-mediated homotypic cell aggregation and endothelial cell morphogenesis. *Glycobiology* **16,** 210–220
16. Cumpstey, I., Sundin, A., Leffler, H., and Nilsson, U. J. (2005) C2-symmetrical thiodigalactoside bis-benzamido derivatives as high-affinity inhibitors of galectin-3: efficient lectin inhibition through double arginine-arene interactions. *Angew. Chem. Int. Ed. Engl.* **44,** 5110–5112
17. Tejler, J., Skogman, F., Leffler, H., and Nilsson, U. J. (2007) Synthesis of galactose-mimicking 1H-(1,2,3-triazol-1-yl)-mannosides as selective galectin-3 and 9N inhibitors. *Carbohyd. Res.* **342,** 1869–1875
18. Nangia-Makker, P., Hogan, V., Honjo, Y., Baccarini, S., Tait, L., Bresalier, R., and Raz, A. (2002) Inhibition of human cancer cell growth and metastasis in nude mice by oral intake of modified citrus pectin. *J. Natl. Cancer Inst.* **94,** 1854–1862
19. Sathisha, U. V., Jayaram, S., Harish Nayaka, M. A., and Dharmesh, S. M. (2007) Inhibition of galectin-3 mediated cellular interactions by pectic polysaccharides from dietary sources. *Glycoconj. J.* **24,** 497–507
20. Streetly, M. J., Maharaj, L., Joel, S., Schey, S. A., Gribben, J. G., and Cotter, F. E. (2010) GCS-100, a novel galectin-3 antagonist, modulates MCL-1, NOXA, and cell cycle to induce myeloma cell death. *Blood* **115,** 3939–3948
21. Vayssade, M., Sengkhamparn, N., Verhoef, R., Delaigue, C., Goundiam, O., Vigneron, P., Voragen, A. G., Schols, H. A., and Nagel, M. D. (2010) Antiproliferative and proapoptotic actions of okra pectin on B16F10 melanoma cells. *Phytother. Res.* **24,** 982–989
22. Pienta, K. J., Naik, H., Akhtar, A., Yamazaki, K., Replogle, T. S., Lehr, J., Donat, T. L., Tait, L., Hogan, V., and Raz, A. (1995) Inhibition of spontaneous metastasis in a rat prostate cancer model by oral administration of modified citrus pectin. *J. Natl. Cancer Inst.* **87,** 348–353
23. Inohara, H., and Raz, A. (1994) Effects of natural complex carbohydrate (citrus pectin) on murine melanoma cell properties related to galectin-3 functions. *Glycoconj. J.* **11,** 527–532
24. Glinsky, V. V., and Raz, A. (2009) Modified citrus pectin anti-metastatic properties: one bullet, multiple targets. *Carbohyd. Res.* **344,** 1788–1791
25. Demotte, N., Wieërs, G., Van Der Smissen, P., Moser, M., Schmidt, C., Thielemans, K., Squifflet, J.L., Weynand, B., Carrasco, J., Lurquin, C., Courtoy, P.J., and van der Bruggen, P. (2010) A galectin-3 ligand corrects the impaired function of human CD4 and CD8 tumor-infiltrating lymphocytes and favors tumor rejection in mice. *Cancer Res.* **70,** 7476–7488
26. Clark, M.C., Pang, M., Hsu, D.K., Liu, F.T., de Vos, S., Gascoyne, R.D., Said, J., and Baum, L.G. (2012) Galectin-3 binds to CD45 on diffuse large B-cell lymphoma cells to regulate susceptibility to cell death. *Blood* **120,** 4635–4644
27. Chauhan, D., Li, G., Podar, K., Hideshima, T., Neri, P., He, D., Mitsiades, N., Richardson, P., Chang, Y., Schindler, J., Carver, B., and Anderson, K.C. (2005) A novel carbohydrate-based therapeutic GCS-100 overcomes bortezomib resistance and enhances dexamethasone-induced apoptosis in multiple myeloma cells. *Cancer Res.* **65,** 8350–8358
28. Wang, Y., Nangia-Makker, P., Balan, V., Hogan, V., and Raz, A. (2010) Calpain activation through galectin-3 inhibition sensitizes prostate cancer cells to cisplatin treatment. *Cell Death Dis.* **1,** e101
29. Maxwell, E. G., Belshaw, N. J., Waldron, K. W., and Morris, V. J. (2012) Pectin—an emerging new bioactive food polysaccharide. *Trends Food Sci. Tech.* **24,** 64–73
30. Gunning, A. P., Bongaerts, R. J., and Morris, V. J. (2009) Recognition of galactan components of pectin by galectin-3. *FASEB J.* **23,** 415–424
31. Gao, X., Zhi, Y., Zhang, T., Xue, H., Wang, X., Foday, A. D., Tai, G., and Zhou, Y. (2012) Analysis of the neutral polysaccharide fraction of MCP and its inhibitory activity on galectin-3. *Glycoconj J* **29,** 159–165
32. Zhang, X., Yu, L., Bi, H., Li, X., Ni, W., Han, H., Li, N., Wang, B., Zhou, Y., and Tai, G. (2009) Total fractionation and characterization of the water-soluble polysaccharides isolated from *Panax ginseng* C. A. Meyer. *Carbohyd. Polym.* **77,** 544–552
33. Fan, Y., Cheng, H., Li, S., Wang, J., Liu, D., Hao, M., Gao, X., Fan, E., Tai, G., and Zhou, Y. (2010) Relationship of the inhibition of cell migration with the structure of ginseng pectic polysaccharides. *Carbohyd. Polym.* **81,** 340–347
34. Yu, L., Zhang, X., Li, S., Liu, X., Sun, L., Liu, H., Iteku, J., Zhou, Y., and Tai, G. (2010) Rhamnogalacturonan I domains from ginseng pectin. *Carbohyd. Polym.* **79,** 811–817
35. Levi, G., and Teichberg, V. I. (1981) Isolation and physicochemical characterization of electrolectin, a β-D-galactoside binding lectin from the electric organ of *Electrophorus electricus*. *J. Biol. Chem.* **256,** 5735–5740

36. Gao, X., Liu, D., Fan, Y., Li, X., Xue, H., Ma, Y., Zhou, Y., and Tai, G. (2012) The two endocytic pathways mediated by the carbohydrate recognition domain and regulated by the collagen-like domain of galectin-3 in vascular endothelial cells. *PLoS One* **7,** e52430
37. ØBro, J., Harholt, J., Scheller, H. V., and Orfila, C. (2004) Rhamnogalacturonan I in *Solanum tuberosum* tubers contains complex arabinogalactan structures. *Phytochemistry* **65,** 1429–1438
38. Deng, C., O'Neill, M. A., Hahn, M. G., and York, W. S. (2009) Improved procedures for the selective chemical fragmentation of rhamnogalacturonans. *Carbohyd. Res.* **344,** 1852–1857
39. Cheng, H., Li, S., Fan, Y., Gao, X., Hao, M., Wang, J., Zhang, X., Tai, G., and Zhou, Y. (2011) Comparative studies of the antiproliferative effects of ginseng polysaccharides on HT-29 human colon cancer cells. *Med. Oncol.* **28,** 175–181
40. Platt, D., and Raz, A. (1992) Modulation of the lung colonization of B16-F1 melanoma cells by citrus pectin. *J. Natl. Cancer Inst.* **84,** 438–442
41. Yu, L., Zhou, Y., and Knox, J. P. (2011) Ginseng root water-extracted pectic polysaccharides originate from secretory cavities. *Planta* **234,** 487–499
42. Bi, H., Ni, X., Liu, X., Iteku, J., Tai, G., Zhou, Y., and Zhao, J. (2009) A novel water-soluble β-(1→6)-D-glucan isolated from the fruit bodies of *Bulgaria inquinans* (Fries). *Carbohyd. Res.* **344,** 1254–1258
43. Glinsky, V. V., Glinsky, G. V., Glinskii, O. V., Huxley, V. H., Turk, J. R., Mossine, V. V., Deutscher, S. L., Pienta, K. J., and Quinn, T. P. (2003) Intravascular metastatic cancer cell homotypic aggregation at the sites of primary attachment to the endothelium. *Cancer Res.* **63,** 3805–3811
44. Stowell, S. R., Arthur, C. M., Mehta, P., Slanina, K. A., Blixt, O., Leffler, H., Smith, D. F., and Cummings, R. D. (2008) Galectin-1, -2, and -3 exhibit differential recognition of sialylated glycans and blood group antigens. *J. Biol. Chem.* **283,** 10109–10123